Results & Discussion

If I have seen further than others, it is by standing upon the shoulders of giants

Newton Isaac

3. RESULTS & DISCUSSION

3.1. 5-Phenyl and 5-benzyl 1,3-dioxane-2-carboxylic acid derivatives as PPARα/γ dual agonists [205, 206]

3.1.1. Chemistry

In the previous section the rationale for designing PPARα/γ dual agonists containing 1,3-dioxane-2-carboxylic acid as pharamacophore has been described, wherein we intended to synthesize the compounds represented by general structures **9** and **15** (**Figure 16**). Synthetic methodology was designed based on the retrosynthetic analysis and the schemes described below. Synthetic methods reported in literature were adapted for the synthesis of **4** and **13** which were the common intermediates for the synthesis of the compounds represented by the **9** and **15** respectively. Oxazole containing fragments were also synthesized following the procedures reported earlier by choosing the suitable starting materials and varying reaction conditions as described in schemes and experimental section.

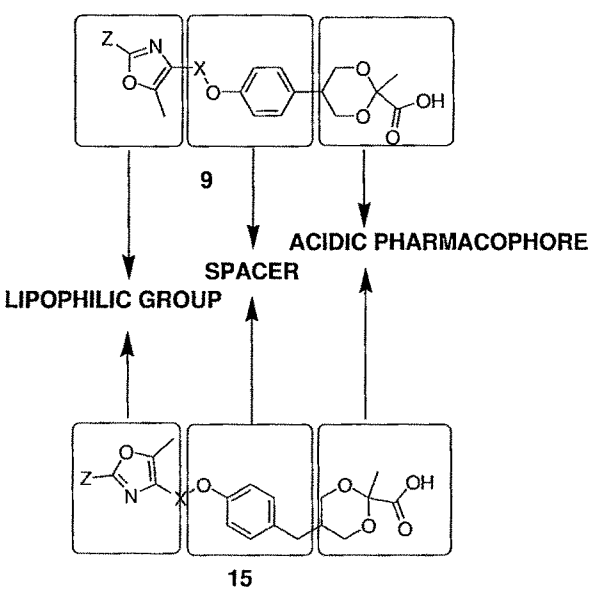

Figure 16. Structural design of novel oxazole containing 1, 3-dioxane2-carboxylic acids

Synthesis of Compounds **9** and **15** is illustrated in **Schemes 1-4**. Synthesis of **4** is outlined in **Scheme 1**. Diester **2** was synthesized by reacting **1** with diethylcarbonate in presence of base, which was reduced to diol **3**. Dioxane ring formation was brought about by the reaction of **3** with methyl pyruvate in the presence of $BF_3.OEt_2$ [**207**, **208**] which gave the cyclized compound as a mixture of geometrical isomers. Carboxyl group prefers the axial orientation in 2- carboxyl 1, 3-dioxane compounds due to the anomeric effect [**209**] and hence two isomers (*trans* isomer in which 2- carboxyl and 5-phenyl are oriented axially and *cis* isomer where the 2-carboxylic is axially oriented where as 5-phenyl is oriented equatorially). These isomers were separated by means of column chromatography to give *cis* isomer **4a** and *trans* isomer **4b.** Both of these isomers showed ^{1}HNMR chemical shifts identical with the other 1,3-dioxane derivatives reported [**209**]. Both **4a** and **4b** were subjected to debenzylation under transfer hydrogenation conditions to obtain the corresponding phenolic intermediate **4c** and **4d.**

Scheme 1:

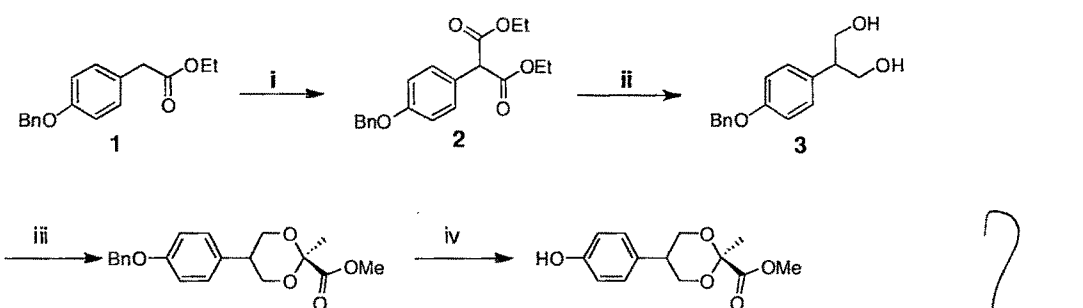

Reagents and conditions: (i) NaH (60 %), Diethyl carbonate, 25 °C, 18 h; (ii) $LiAlH_4$, THF, 25 °C, 6 h; (iii) $MeCOCO_2Me$, $BF_3.OEt_2$, CH_3CN, 25 °C, 4 h; (iv) Pd/C (10 %), ammonium formate, MeOH, reflux, 2 h.

Synthesis of intermediates **7** is illustrated as **Scheme 2** [**210**, **211**]. Reacting the aldehyde **5** with diacetylmonoxime in acetic acid and passing HCl gas gave the intermediate **6** which was treated with $POCl_3$ to obtain chloro

derivatives of **7** where **X** represents a methylene group. Treatment of these compounds with NaCN followed by sulfuric acid in ethanol gave the corresponding esters which were reduced to hydroxy compounds and treated with methanesulphonyl chloride to yield the corresponding mesylate derivatives **7** wherein **X** represents ethylene group. Compound **7e** was synthesized from **7b** in four steps. The compound **7b** was reacted with diethylmalonate in the presence of sodium hydride and then hydrolyzed and decarboxylated. The mono carboxylic acid so obtained was reduced to the corresponding hydroxy derivative which was subsequently converted to its mesylate derivative **7e**.

Scheme 2:

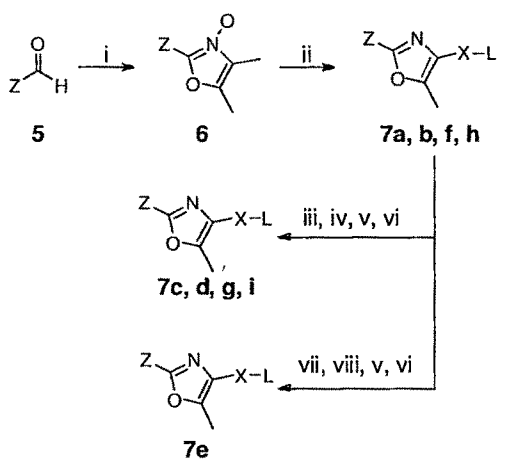

	X	Z	L
a	CH_2	Phenyl	Cl
b	CH_2	4-methylphenyl	Cl
c	$(CH_2)_2$	phenyl	OSO_2CH_3
d	$(CH_2)_2$	4-methylphenyl	OSO_2CH_3
e	$(CH_2)_3$	4-methylphenyl	OSO_2CH_3
f	CH_2	5-methylthiophene-2yl	Cl
g	$(CH_2)_2$	5-methylthiophene-2yl	OSO_2CH_3
h	CH_2	*t*-Butyl	Cl
i	$(CH_2)_2$	*t*-Butyl	OSO_2CH_3

Reagents and conditions: (i) Diacetylmonooxime, AcOH, HCl (g), 0-10 °C, 3 h; (ii) $POCl_3$, reflux, 2 h; (iii) NaCN, DMF, 25 °C, 18 h; (iv) EtOH, H_2O, H_2SO_4, reflux, 24 h; (v) $LiAlH_4$, THF, 25 °C, 6 h; (vi) CH_3SO_2Cl, Et_3N, CH_2Cl_2, 0-10 °C, 30 min; (vii) NaH (60 %), Diethyl malonate, 25 °C, 14 h; (viii) NaOH, EtOH, H_2O, reflux, 24 h.

Compounds **9a-d** were synthesized according to the **Scheme 3**. Nucleophilic substitution reaction of the intermediate **4c** with **7a-d** in the presence of K_2CO_3 as a base gave the esters **8a-d**, which upon hydrolysis resulted in the acids **9a-d.** Compound **9e**, the trans isomer of **9d** was prepared from **7d** and **4d** (*trans* isomer) using the similar method described for *cis* isomer **9**.

Scheme 3:

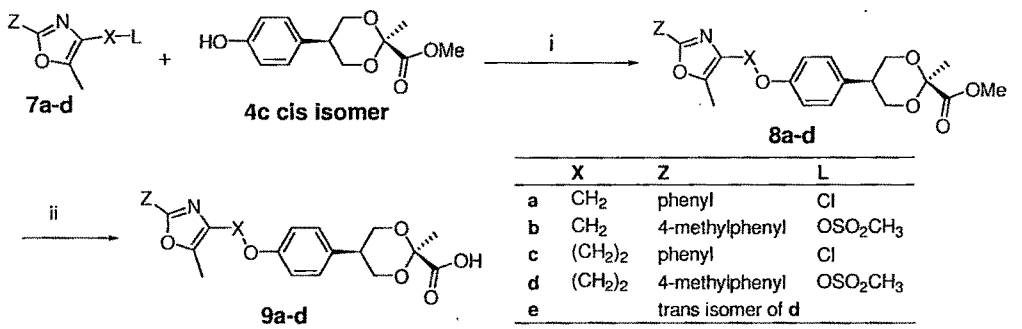

	X	Z	L
a	CH_2	phenyl	Cl
b	CH_2	4-methylphenyl	OSO_2CH_3
c	$(CH_2)_2$	phenyl	Cl
d	$(CH_2)_2$	4-methylphenyl	OSO_2CH_3
e		trans isomer of d	

Reagents and conditions: (i) K_2CO_3, DMF, 60 °C, 18 h; (ii) LiOH, THF, H_2O, MeOH, 25 °C, 18 h.

Scheme 4:

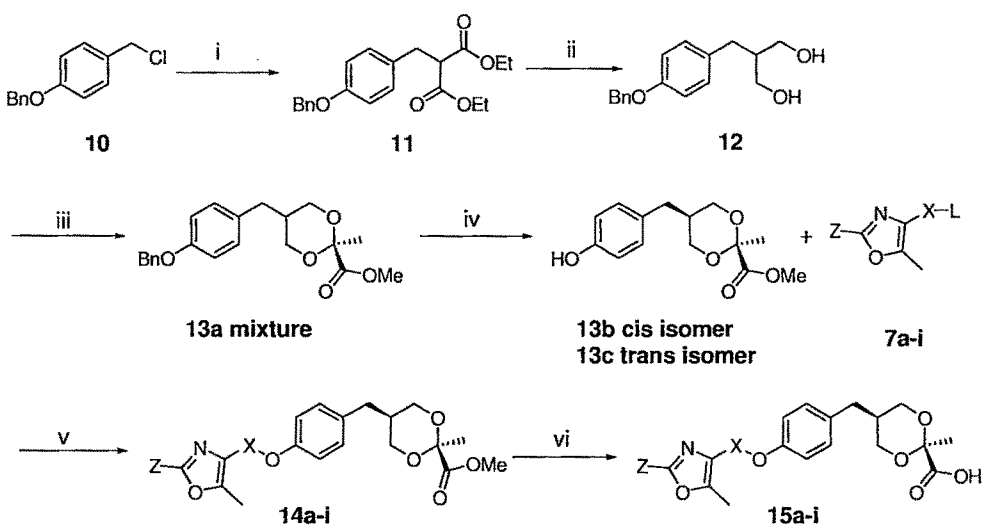

	X	Z	L
a	CH_2	Phenyl	Cl
b	CH_2	4-methylphenyl	Cl
c	$(CH_2)_2$	phenyl	OSO_2CH_3
d	$(CH_2)_2$	4-methylphenyl	OSO_2CH_3
e	$(CH_2)_3$	4-methylphenyl	OSO_2CH_3

	X	Z	L
f	CH_2	5-methylthiophene-2yl	Cl
g	$(CH_2)_2$	5-methylthiophene-2yl	OSO_2CH_3
h	CH_2	*t*-Butyl	Cl
i	$(CH_2)_2$	*t*-Butyl	OSO_2CH_3
j		trans isomer of a	

Reagents and conditions: (i) NaH (60 %), Diethyl malonate, 25 °C, 14 h; (ii) $LiAlH_4$, THF, 25 °C, 6 h; (iii) $MeCOCO_2Me$, $BF_3.OEt_2$, CH_3CN, 25 °C, 4 h; (iv) Pd/C (10 %), ammonium formate, MeOH, reflux, 2 h; (v) K_2CO_3, DMF, 60 °C, 18 h; (vi) LiOH, THF, H_2O, MeOH, 25 °C, 18 h.

Synthesis of compounds **15a-i** is illustrated in **Scheme 4**. Diester **11** was synthesized from **10** by reacting with diethylmalonate in the presence of sodium hydride. Transformation of **11** to cyclized dioxane **13a** (as a mixture of *cis* and

trans isomers) was achieved by the reduction to diol **12** followed by the treatment with methyl pyruvate in the presence of $BF_3.OEt_2$. Surprisingly the attempts to separate the *cis* and *trans* isomers of **13a** by column chromatography were unsuccessful. However separation by recrystalization was successful after debenzylating the mixture of isomers. Pure *cis* isomer **13b** was obtained quantitatively as first crop whereas *trans* isomer **13c** could be obtained only after repeated crystallizations. Coupling of *cis* intermediate **13b** with **7a-i** in the presence of potassium carbonate in DMF furnished the ester derivatives **14a-i**. Hydrolysis of these esters under aqueous alkaline conditions followed by neutralization gave the compounds **15a-i**. Similarly **15j**, the *trans* isomer of **15a** was synthesized by coupling **7a** and **13c**, followed by hydrolysis.

The axial orientation of the carboxyl group in dioxane ring is demonstrated by single crystal X-ray diffraction of the *trans* isomer **13c** (**Figure 17**) and the *cis* isomer **15b** (**Figure 18**). In both the compounds the carboxyl group at 2-position is oriented axially, while the benzyl group at 5-position is oriented axially in **13c** and equatorially in **15b**. These results provide conclusive evidence for the preferred axial orientation of carboxyl group due to anomeric effect as described earlier.

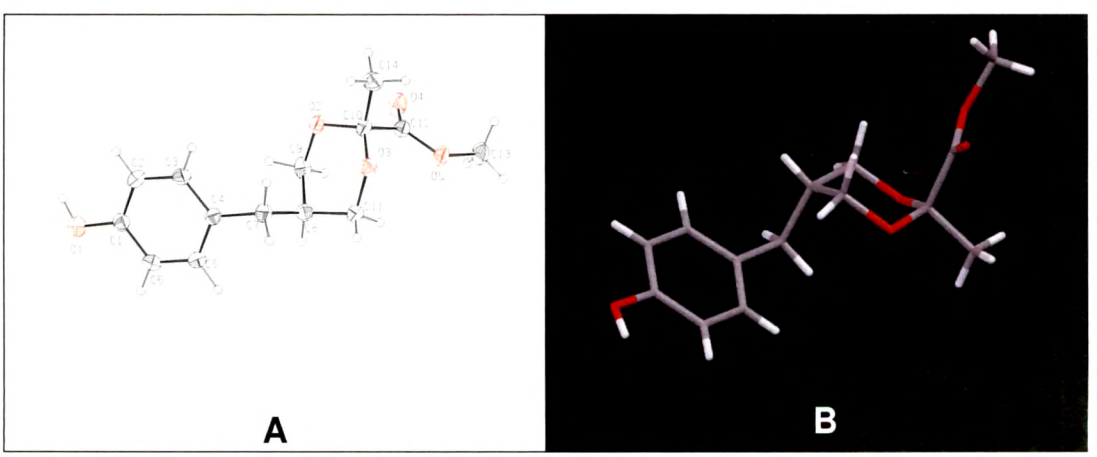

Figure 17. Structure of **13c** determined by single crystal X-ray diffraction: (**A**) ORTEP diagram with atom numbering scheme. (**B**) image generated by Mercury software 2.3 version.

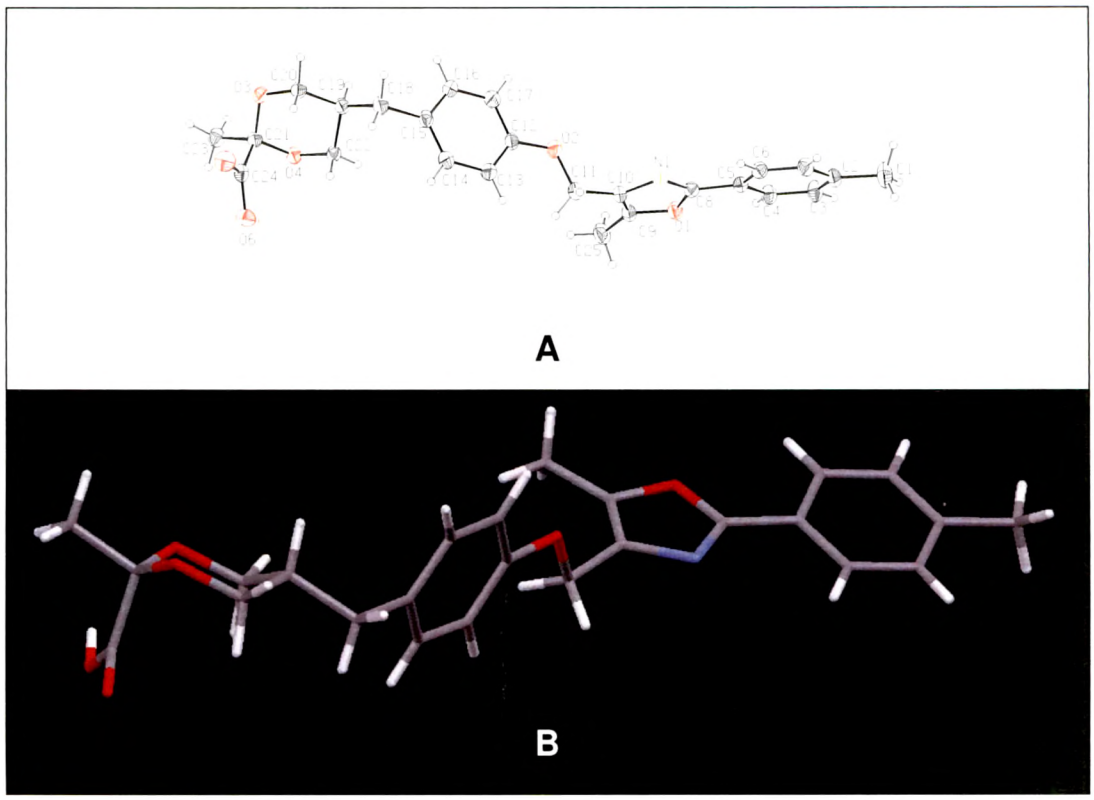

Figure 18. Structure of **15b** determined by single crystal X-ray diffraction: (**A**) ORTEP diagram with atom numbering scheme. (**B**) image generated by Mercury software 2.3 version.

Synthesis of **18a-f** is shown in **Scheme 5**. Intermediates **16a, c** and **d** were synthesized by reacting the corresponding heterocycle with ethyl-2-bromoacetate followed by reduction of ester using $LiAlH_4$ and finally treating the hydroxy compounds with methanesulfonylchloride. Initially these heterocycles were treated with dibromoethane in the presence of a base. Since this method needed strong base like sodamide and the yields were very low, the fore mentioned method was adopted. **16b** was prepared from 2-amino-*N*-methylbenzamide according to the procedures similar to that known in the literature with variations in reaction conditions and reagents [**212**]. **16e** and **16f** were synthesized by reacting the corresponding oxime with dibromoethane in the presence of a base in good yields. The detailed procedures for the preparation of **16a-f** have been described in experimental section. Coupling reaction of **16a-f** with **13b** in the presence of potassium carbonate in DMF gave the esters **17a-f,**

which on hydrolysis under aqueous basic conditions followed by neutralization yielded carboxylic acids **18a-f**.

Scheme 5:

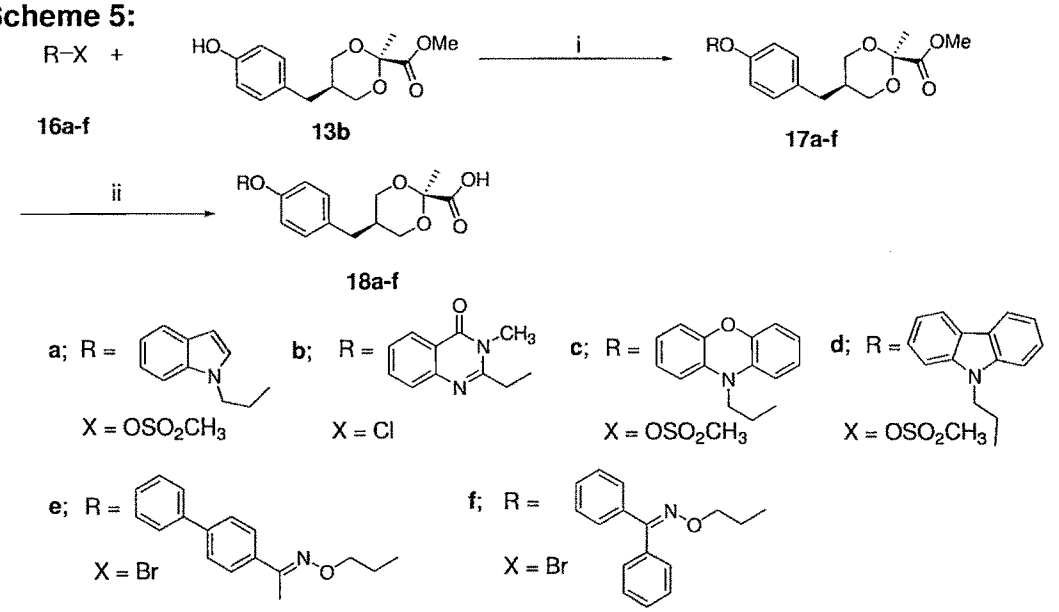

Reagents and conditions: (i) K_2CO_3, DMF, 60 °C, 18 h; (ii) LiOH, THF, H_2O, MeOH, 25 °C, 18 h.

Scheme 6:

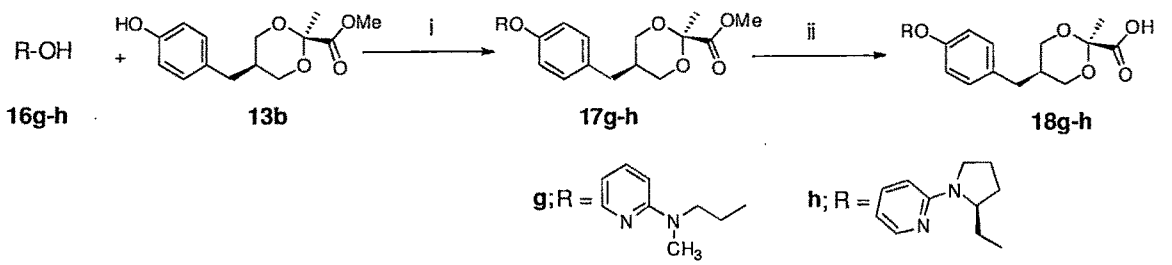

Reagents and conditions: (i) DIAD, Ph_3P, THF, 0-25 °C, 1 h; (ii) LiOH, THF, H_2O, MeOH, 25 °C, 18 h.

Synthesis of **18g** and **18h** is outlined in **Scheme 6**. Hydroxy intermediates **16g** [**213**] and **16h** [**214**] were synthesized according to the methods reported in the literature and are described in the experimental section. Mitsunobu coupling between **16g-h** and **13b** using triphenylphosphine and diisopropyl azodicarboxylate (DIAD) gave the esters **17g-h** which were hydrolysed under

aqueous basic condition to furnish acids **18g-h**. Mitsunobu methodology was adapted since conversion of hydroxy group of **16g** into a leaving group was not successful. In **16h** the prolinol undergoes ring expansion to form piperidinol when the hydroxy group is transformed into a leaving group [**215**].

Compound **18i** was synthesized following the methods described in **Scheme 7**. Coupling reaction between **16i** and **13b** gave the ester, which was debenzylated under transfer hydrogenation conditions to furnish hydroxy compound which upon the treatment with methanesulfonylchloride in the presence of triethylamine gave **17i**. Hydrolysis of **17i** under aqueous basic condition followed by neutralization gave the acid **18i**.

Scheme 7:

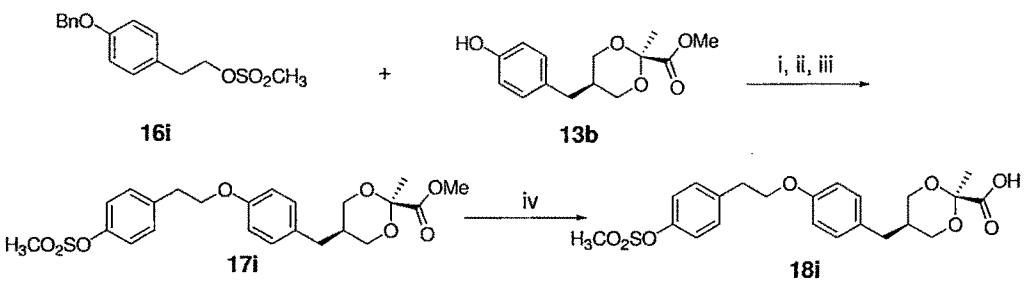

Reagents and conditions: (i) K_2CO_3, DMF, 60 °C, 18 h; (ii) Pd/C (10%), ammonium formate, MeOH, reflux, 2 h; (iii) CH_3SO_2Cl, Et_3N, CH_2Cl_2, 0-10 °C, 30 min; (iv) LiOH, THF, H_2O, MeOH, 25 °C, 18 h.

3.1.2. Biology

All the final compounds **9**, **15** and **18** synthesized were screened for human PPARα, γ and δ agonistic activity on full length PPAR receptor transfected in HepG2 cells. WY-14643, Rosiglitazone and GW-501516 were used as controls for PPARα,γ and δ respectively. The activities are reported as fold activation shown by compounds against the vehicle (DMSO) at one concentration of the test compounds as shown in **Tables 7** and **8**. Based on this fold activation, potent compounds were selected for screening at multiple concentrations and determination of EC_{50}, which is the concentration of the test compound that exhibits half-maximum transactivation activity. The detailed

procedure of *in vitro* experiments was described in the experimental section. The results are summarized in **Tables 7** and **8**.

As described earlier a typical chemical structural design of PPAR ligands comprises of an acidic head as pharmacophore which is connected to an aromatic ring (mostly phenyl) which inturn connected to a lipophilic tail group through a tether like alkoxy group. Initially to start with the synthesis of novel compounds, phenyl dioxane carboxylic acid has been chosen as pharmacophore which contained acidic head connected to phenyl ring mimicking a typical pharmacophore chemotype of PPAR agonist. Then substituted oxazole group has been selected as lipophilic tail for the reason that this heterocycle being used extensively in PPAR drug discovery research (**Figures 5**, **7** & **9**). With this background compounds **9a-d** have been synthesized. Compounds **9a** and **9c** both having phenyl ring at 2-position on oxazole with a tether of methylene and ethylene respectively showed moderate PPARα activity. When the phenyl ring at 2-position on oxazole was substituted with a methyl group at metabolically susceptible *para*-position (compound **9b)** with methylene tether showed similar activity as **9a** but the compound **9d** did not show any PPAR activity. The *trans* isomer of **9e** was also screened to study the effect of conformational difference on biological activity. But this compound was also found to be inactive as well. Since none of the compounds showed superior activity than the control compounds in terms of their fold induction, they have not been evaluated for their EC_{50} values. Then we intended to synthesize compounds **15a-i**, which resembles glitazone structure more closely. Compound **15a** with phenyl ring at 2-position of oxazole and a methylene tether showed an EC_{50} of 0.096 μM towards PPARγ and 1.09 μM towards PPARα, while the compound **15c** with ethylene spacer showed inferior and contradictory results with 0.27 μM and 4.1 μM towards PPARα and PPARγ respectively. When the phenyl ring in compounds **15a** and **15c** was substituted with a methyl group at *para* position the respective resulting compounds **15b** and **15d** exhibited superior activity compared to parent compounds and surprisingly compound **15b** was found equipotent towards

PPARα and γ with 0.07 μM and 0.015 μM EC_{50} respectively. The further elongation of the tether to propylene group as in compound **15e** found detrimental to PPAR affinities. Having done this, we wanted to replace the phenyl ring on oxazole with 5-methyl thiophene which was selected from a lead compound of our in-house library and the resulting compounds **15f** and **15g** showed interesting PPAR activity. **15f** found to be 30 fold more selective towards PPARγ where as **15g** was 8 fold more selective towards PPARα. Replacing phenyl ring with *tert*-butyl group rendered the compounds **15h** and **15i**, both of which exhibited poor activation towards PPARα andγ. The *trans* isomer **15j** was also found to be inferior to its corresponding cis isomer **15a**. These results could demonstrate the viability of our approach towards developing novel PPARα/γ dual agonists.

Table 7

in vitro hPPAR transactivation data of compounds **9** and **15**

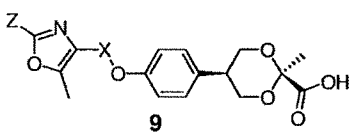

9

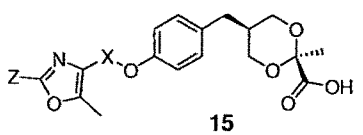

15

Compound	X	Z	hPPAR Transactivation[a]				
			α[b] (10μM)	γ[b] (0.2μM)	δ[b] (10μM)	$EC_{50}\alpha$ (μM)	$EC_{50}\gamma$ (μM)
9a	methylene	phenyl	3.0	1.6	1.4	ND	ND
9b	methylene	4-methylphenyl	2.7	1.5	1.2	ND	ND
9c	ethylene	phenyl	3.0	1.5	1.3	ND	ND
9d	ethylene	4-methylphenyl	IA	1.6	1.5	ND	ND
9e	*trans* isomer of **9d**		IA	1.5	IA	ND	ND
15a	methylene	phenyl	6.5	11.4	1.7	1.09	0.096
15b	methylene	4-methylphenyl	8.2	12.7	IA	0.072	0.015
15c	ethylene	phenyl	5.3	3.9	IA	0.272	4.096
15d	ethylene	4-methylphenyl	6.3	3.4	IA	0.089	1.385
15e	*n*-propylene	4-methylphenyl	1.8	1.8	IA	ND	ND
15f	methylene	5-methyl thiophen-2yl	5.6	11.5	IA	0.6	0.0198

Compound	X	Z	hPPAR Transactivation[a]				
			α[b] (10μM)	γ[b] (0.2μM)	δ[b] (10μM)	$EC_{50}\alpha$ (μM)	$EC_{50}\gamma$ (μM)
15g	ethylene	5-methyl thiophen-2yl	6.8	8.9	1.1	0.03	0.239
15h	methylene	*tert*-Butyl	2.3	3.2	IA	ND	ND
15i	ethylene	*tert*-Butyl	5.8	4.2	1.2	4.2	5.01
15j	*trans* isomer of **15a**		4.5	3.3	IA	ND	ND
Vehicle (DMSO)			1.0	1.0	1.0	-	-
WY-14643			4.4	ND	ND	4.8	ND
Rosiglitazone			ND	11.6	ND	ND	0.05
GW-501516@ 2 nM			ND	ND	4.3	ND	ND

[a] IA denotes inactive where compounds did not show any fold induction above the basal level shown by vehicle and ND denotes not determined. hPPAR denotes human PPAR.

[b] Activities are presented as fold induction of PPARα, γ and δ activation over the basal level (DMSO).

Encouraged with the *in vitro* activity of compounds **15**, in order to synthesize further compounds with this novel pharmacophore, our goal was to modify the lipophilic tail part by replacing the oxazole moiety in compound **15** with different moieties as depicted in **Figure 19**.

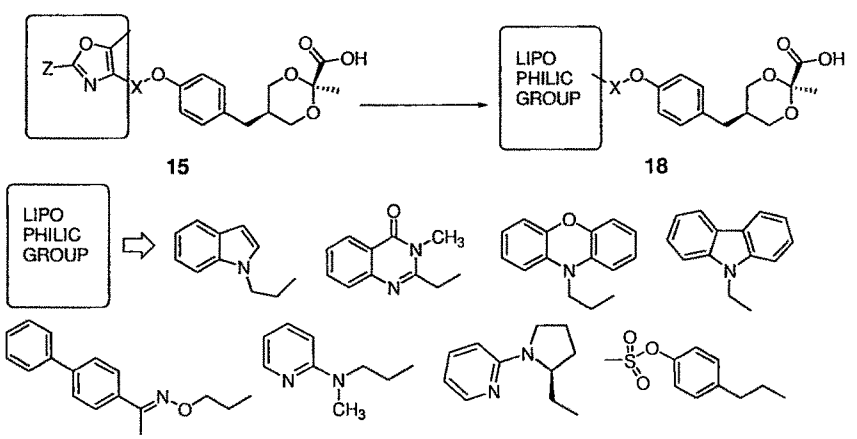

Figure 19. Structural modifications in lipophilic tail region. Oxazole group in compounds **15** is replaced with lipophilic groups of potent PPAR agonists.

To achieve this lipophilic part of few lead compounds reported in the literature are selected and compounds **18a-i** were synthesized and evaluated for their *in vitro* PPAR activation potential and *in vivo* triglyceride (TG) lowering activity in *Swiss albino mice*, A moderately hyperlipidemic model. Compound **18a** was first synthesized using indole as a lipophilic tail, based on a known compound DRF-2189 [**216**] and is found to be selective PPARα activator and reduced serum triglycerides (TG) by 42% in *Swiss albino mice*, a moderately hyperlipidemic model generally used to study the TG lowering effect. The use of *N*-methylaminopyridine and pyrrolidinopyridine present in Rosiglitazone and one of our previously reported compound [**214**] respectively led to the compounds **18g** and **18h.** Both of these compounds were found inactive *in vitro* as well as *in vivo* in reducing TG. Compound **18i** in which 4-methanesulfonyloxyphenyl group of Tesaglitazar was used as tail is also found to be a weak PPARα agonist. Based on these results and in order to improve PPARγactivation we then wanted to synthesize the compounds with bulky tail groups as ligand-binding pocket of PPAR$\gamma$is bulkier than that of PPARα. This led us to synthesize the compounds **18b**, **18c** and **18e** possessing the heterocyclic groups of Balaglitazone **[170]**, Ragaglitazar [**178**] and its carbazole analogue [**217**] respectively. **18b** and **18c** are found inactive both *in vitro* and *in vivo*, whereas **18d** has been found to be a weak PPARα agonist with no activation towards $\gamma$and marginally reduced TG by 16%. The lipophilic tails used in all of the above compounds were well optimized and as they do not work in combination with our pharmacophore, we looked for some suitable groups and we observed a series of compounds containing substituted oxime as a lipophilic tail where the lead compound 5-{4-[2-(1-Biphenyl-4-yl-ethylideneaminooxy)-ethoxy]-benzyl}-thiazolidine-2,4-dione possesses 1-biphenyl-4-yl-ethanone oxime as a lipophilic tail [**218**]. Thus **18e** containing 1-biphenyl-4-yl-ethanone oxime was synthesized and as expected this compound has turned out to be a very potent PPARα/γ dual agonist. However this compound is not effective in reducing TG *in vivo*. Further high *in vitro* potency also raises safety concerns based on our earlier experience with highly

potent PPAR agonists. Molecular modeling experiments conducted on **18e** revealed that biphenyl group is responsible for its high potency towards PPARα and when the terminal phenyl group is removed and substituted for the methyl group the resulting compound **18f** showed accurate fitting in the pockets of both PPARα and γ with equal affinity. Subsequently compound **18f** was synthesized and evaluated for its PPAR activation where it exhibited moderate and equal potency towards PPARα and γ with an EC_{50} of 0.14 and 0.75 µM. This compound also reduces serum TG by 46 % when administered to *Swiss albino* mice (SAM).

Table 8

in vitro hPPAR transactivation and Serum triglyceride lowering activity of compounds **18**

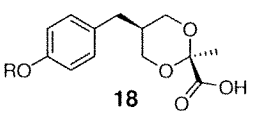

18

Compound	R	hPPAR transactivation[a]					% Change in TG in SAM[c]
		α^b (10µM)	γ^b (0.2µM)	δ^b (10µM)	$EC_{50}\alpha$ (µM)	$EC_{50}\gamma$ (µM)	
18a	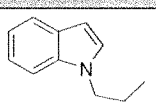	10.4	2.05	IA	0.15	5.10	-42
18b	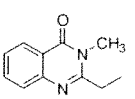	1.4	0.7	1.5	ND	ND	IA
18c	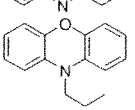	3.8	1.8	2.0	ND	ND	IA
18d	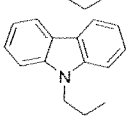	4.4	1.19	2.78	0.54	ND	-16
18e	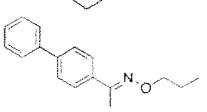	8.8	10.4	1.4	0.0002	0.02	-9
18f	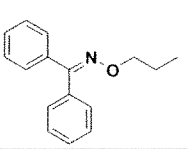	9.8	1.57	IA	0.14	0.75	-46

Compound	R	hPPAR transactivation[a]					% Change in TG in SAM[c]
		α^b (10μM)	γ^b (0.2μM)	δ^b (10μM)	$EC_{50}\alpha$ (μM)	$EC_{50}\gamma$ (μM)	
18g	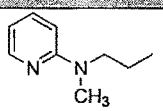	3.9	1.2	0.9	ND	ND	IA
18h	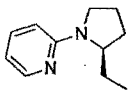	1.2	1.3	IA	ND	ND	IA
18i	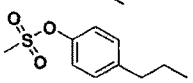	7.2	1.36	1.1	3.2	53	-30
Vehicle		1.0	1.0	1.0	-	-	-
WY-14643		4.4	ND	ND	4.8	ND	ND
Rosiglitazone		ND	11.6	ND	ND	0.05	ND
GW-501516@ 2 nM		ND	ND	4.3	ND	ND	ND

[a] IA denotes inactive where compounds did not show any fold induction above the basal level shown by vehicle and ND denotes not determined. hPPAR denotes human PPAR.

[b] Activities are presented as fold induction of PPARα, γ and δ activation over the basal level (DMSO).

[c] Values indicated are the mean of n=6 animals and $p < 0.05$ vs vehicle control.

Based on these results, compound **15b** & **18f** which were found equally potent towards PPARα & γ and **18a** which reduced serum TG by 42% though exhibited poor PPAR activation *in vitro*, were selected as the lead compounds and their pharmacokinetic behavior was studied in male *Wistar* rats and the results are summarized in **Table 9**. Compound **15b** exhibits excellent oral absorbance at a dose of 30 mg/kg with a maximum plasma concentration (C_{max}) of 54 μg/mL and area under the curve (AUC) of 351 h.μg/mL. (AUC) of 351 h.μg/mL. Compound **18a** also shows high absorbance though inferior to **15b**. While compound **18f** is found to be inferior to both **15b** and **18a** in terms of both C_{max} and AUC.

Table 9

Pharmacokinetic parameters[a] of **15b**, **18a** and **18f** in male *Wistar* rats

Compound	Route	dose (mg/kg)	T_{max} (h)	C_{max} (μg/mL)	$T_{1/2}$ (h)	AUC(0-∞) (h.μg/mL)
15b	Oral	30	1.7	54	2.7	351
18a	Oral	30	2.0	16.58	4.08	59.76
18f	Oral	30	1.4	2.6	3.8	11.9

[a] Values indicated are the mean of n=6 animals and $p < 0.05$ vs vehicle control.

These results indicate that all the three compounds possess favorable pharmacokinetic profiles and can be further evaluated for their anti diabetic and dyslipidemic activities in animal models.

Subsequently **15b, 18a and 18f** were tested in *db/db* mice, a model characterized by early hyperinsulinemia with marked hyperglycemia progressing with age to slowly developing islet failure for their hypolipidemic and anti-hyperglycemic activities and the results are summarized in **Table 10**.

Table 10

in vivo efficacy of the compound **15b**, **18a** and **18f** in *db/db* mice[a]

Compound	Dose (mg/kg/day)	% Change	
		TG	Glucose
15b	3	-50	-57
18a	3	-49	-52
18f	3	-51	-28
Rosiglitazone	30	-41	-54
Tesaglitazar	3	-60	-54

[a] Values indicated are the mean of n=6 animals and $p < 0.05$ vs vehicle control.

When dosed orally to *db/db* mice at a dose of 3mg/kg/day for 6 days, **15b** reduced serum glucose by 57% and triglycerides (TG) by 50%. **18a** though inferior to **15b** both *in vitro* and in pharmacokinetic profile, reduced glucose and TG to a similar extent by 49% and 52% respectively. **18f** though reduced TG by

51% which is comparable to other two compounds, surprisingly is found to be not as effective as either of the two compounds in reducing glucose probably due to poor absorbance compared to the other two compounds and low fold induction towards PPARγ *in vitro*.

Based on these results **15b** was further evaluated in Zucker *fa/fa* rats, a secondary animal model of metabolic syndrome. **15b** when administered orally to male Zucker *fa/fa* rats at a dose of 3mg/kg/day for 14 days normalized glucose tolerance and significantly reduces fasted serum insulin to an extent of 77%. Additionally **15b** reduced serum TG by 71% and serum total cholesterol (TC) by 30% (**Table 11**). The above results indicate that compound **15b** shows hypoglycemic, hypolipidemic and insulin sensitizing effects comparable to Rosiglitazone and Tesaglitazar.

Table 11

in vivo efficacy of the compound **15b** in Zucker *fa/fa* rats[a]

Compound	Dose (mg/kg/day)	% Change			% Improvement in Glucose AUC
		TG	TC	Fasted insulin	
15b	3	-71	-30	-77	51
Rosiglitazone	30	-57	-17	-78	49
Tesaglitazar	3	-67	-16	-91	51

[a] Values indicated are the mean of n=6 animals and $p < 0.05$ vs vehicle control

3.1.3. Molecular docking study

For a better understanding of the activity of **15b**, **18a** and **18f** at molecular level, docking simulations were carried out for these compounds using Discovery Studio software version 1.6. The geometry of compound docked was subsequently optimized using the CHARMM force field. The energy minimization was carried out using smart minimizer option in the software until the gradient value was smaller than 0.001 kcal/ mol A°.

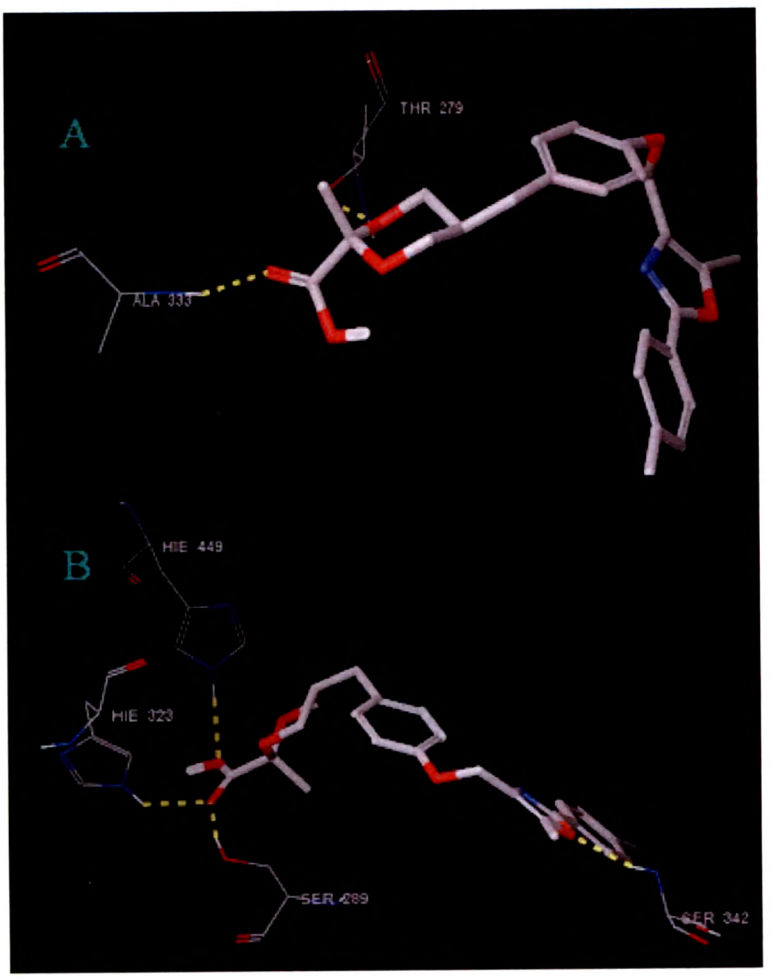

Figure 20. Models of **15b** docked into PPARα (**A**) and γ (**B**) binding site. *H*-bond interactions with amino acids are shown as dashed lines.

The complexed X-ray crystal structure of the ligand binding domain (LBD) of PPARα with GW409544 (1k7l.pdb) [**19**] and PPARγ with Rosiglitazone (2PRG.pdb) were obtained from RCSB Protein Data Bank. When docked into PPARα binding pocket the most stable docking model of **15b** adopts a conformation that allows the carboxylic group to form hydrogen bond with Ala333 and oxygen of dioxane to form hydrogen bond with Thr279. (**Figure 20A**) Whereas in PPARγ binding pocket **15b** adopts a conformation that allows

the carboxylic group to form hydrogen bonds with His 323, and Ser289, and are reported H-bond interaction for a PPAR γ agonist (**Figure 20B**).

Similarly **18a** adopts a conformation that allows the carboxylic group to form hydrogen bond with Tyr464. Other important reported residue Ser280 is very close to the ligand (**Figure 21A**). When docked into PPARγ binding pocket, **18a** adopts a conformation that allows the carboxylic group to form hydrogen bonds with His323, and Ser289 while other important residues Tyr473, Gln286 are very close to ligand (**Figure 21B**).

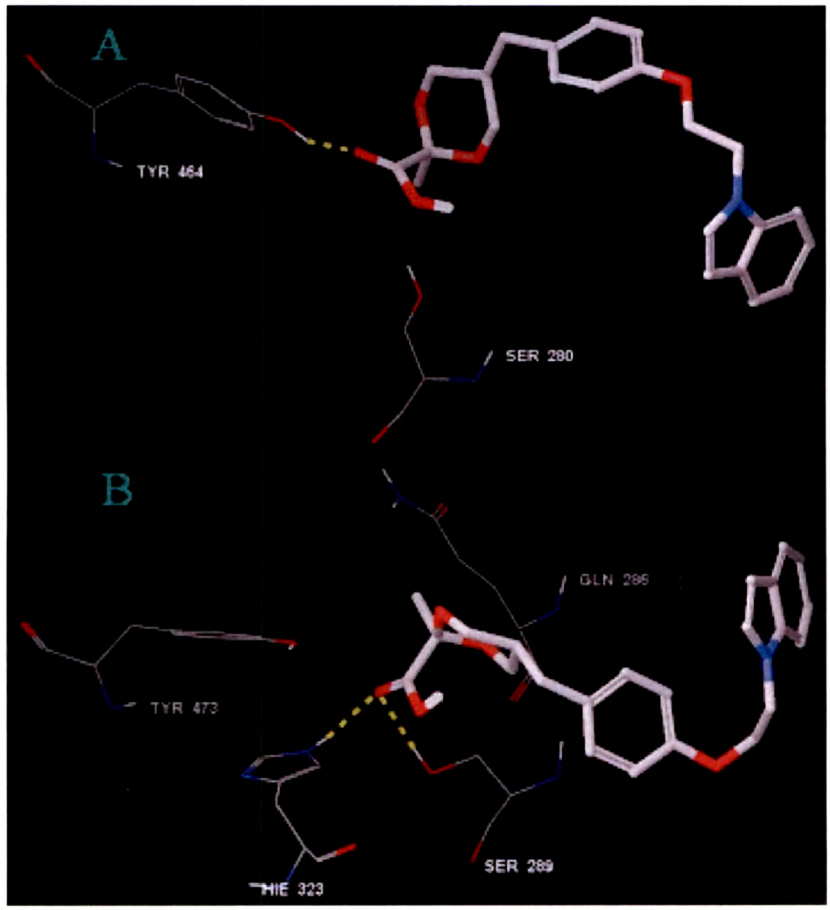

Figure 21. Models of **18a** docked into PPARα (**A**) and γ (**B**) binding site. *H*-bond interactions with amino acids are shown as dashed lines.

18f when docked into PPARα binding pocket adopts a conformation that allows the carboxylic group to form hydrogen bonds with Tyr314, Tyr464, and Ser280 (**Figure 22A**), Whereas in PPARγ binding pocket the carboxylic group of **18f** forms hydrogen bonds with Tyr473, and Ser289. His223 and Gln286 are very close to ligand which were also reported to be essential (**Figure 22B**).

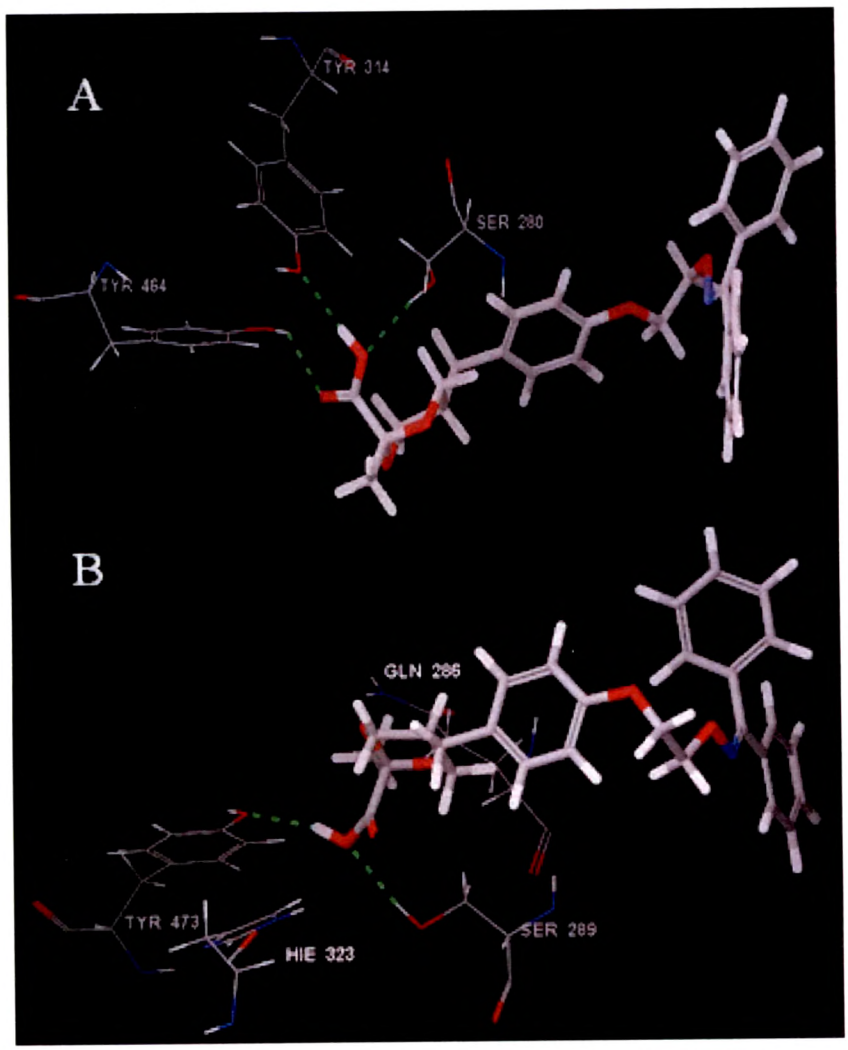

Figure 22. Models of **18f** docked into PPARα (**A**) and γ (**B**) binding site. *H*-bond interactions with amino acids are shown as dashed lines.

3.2. 5-Alkyl 1,3-dioxane-2- carboxylic acid derivatives as PPARα agonists [219]

After identifying a potent and efficacious PPARα/γ dual agonist, we then decided to synthesize a few compounds as selective PPARα agonists as recent research findings suggest that even selective PPARα agonists can be useful in treating the abnormalities in lipid as well as glucose metabolism. While we were engaged in developing the compounds containing 1,3-dioxane-2-carboxylic acid as PPARα/γ dual agonist, scientists at Nippon Shinayaku reported a series of compounds containing same acidic head as selective PPARα agonists and the lead compound NS-220 was found to be very efficacious in reducing both glucose and lipids [**220**]. Though this compound is very potent and efficacious, its development is discontinued for unknown reasons. We believed the potency of this compound as a possible reason for its failure and further, we intended to synthesize compounds with moderate potency and desired efficacy. To meet this objective we designed the compounds **26** and **32** based on hybridization strategy as described in the previous section.

3.2.1. Chemistry

Synthesis of the compounds represented by the general structures **26** and **32** is described in **Schemes 8**, **9** and **10**.

The synthesis of compounds **26a-f** is outlined in **Scheme 8**. Starting materials **19a-e**, synthesized by the Friedel-Crafts acylation of suitably substituted benzene with succinic anhydride [**221**] were reduced initially with Zn/Hg to furnish the compounds **20a-e** which were further reduced with $LiAlH_4$ to yield the hydroxy compounds **25a-e**. Compound **21f** was prepared from **20d** as follows. **20d** was demethylated using HBr in AcOH, esterified and the phenolic hydroxy was benzylated to yield the compound **20f** which was then reduced with $LiAlH_4$ to yield the hydroxy compound **21f**. These compounds **21a-f** were converted to their corresponding mesylate derivatives **22a-f** and treated with diethylmalonate in the presence of sodium hydride to yield diesters **23a-f**. These

diesters were reduced with $LiAlH_4$ to the diols **24a-f**. **24a-f** when reacted with methylpyruvate in the presence of $BF_3.OEt_2$ complex in acetonitrile cyclized to yield **25a-f** as a mixture of geometric isomers. The mixture was separated by chromatography to get the *cis*-isomers **25a-f** which show the chemical shift pattern in ^{1}HNMR identical to that of the other *cis* derivatives described earlier. These esters **25a-f** were hydrolyzed using aqueous LiOH followed by neutralization to obtain the acids **26a-f**.

Scheme 8:

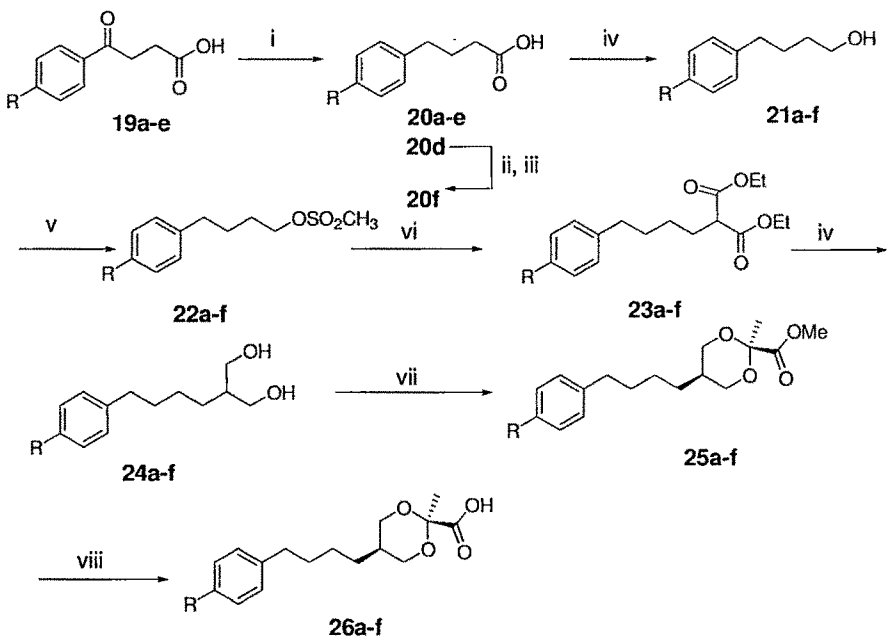

Reagents and Conditions: (i) Zn/Hg, Toluene, AcOH, H_2O, reflux, 4 h; (ii) HBr/AcOH, (iii) BnBr, K_2CO_3, DMF, 30 °C, 6 h (iv) $LiAlH_4$, THF, 0-10 °C, 1 h; (v) CH_3SO_2Cl, Et_3N, CH_2Cl_2, 0-10 °C, 30 min; (vi) Diethyl malonate, NaH, THF, 60 °C, 48 h; (vii) $MeCOCO_2Me$, $BF_3.OEt_2$, CH_3CN, 25 °C, 2 h; (viii) LiOH, H_2O, THF, MeOH, 25 °C, 18 h.

Compounds **26g** and **26h** were synthesized as illustrated in **Scheme 9**. Sulfanyl derivative **25c** when treated with 1.2 molar equivalent of *m*-CPBA gave the corresponding sulfinyl derivative which on hydrolysis followed by neutralization gave the acid **26g** where as the same compound **25c** on treatment

with 3 molar equivalents of *m*-CPBA gave the sulfonyl derivative **25h** which upon hydrolysis followed by neutralization yielded the acid **26h**.

Scheme 9:

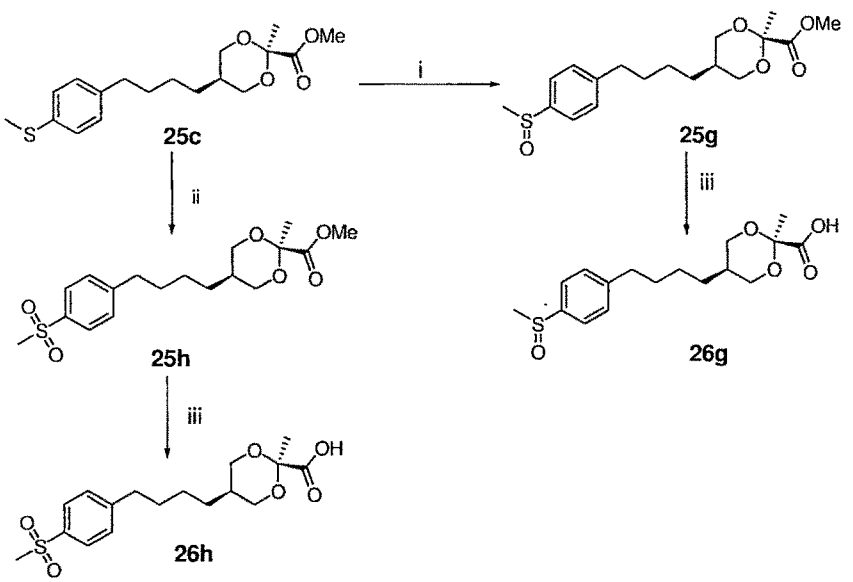

Reagents and Conditions: (i) *m*-CPBA (1.2 equiv.), $CHCl_3$, 0-10 °C, 30 min; (ii) *m*-CPBA (3 equiv.), $CHCl_3$, 25 °C, 1 h; (iii) LiOH, THF, MeOH, 25 °C, 18 h.

Scheme 10 illustrates the synthesis of **26j**, **32a** and **32b**. Diester **27** was prepared by reacting 3-(4-benzyloxyphenyl) propylmethane sulfonate with diethylmalonate in the presence of sodium hydride. **27** and **23f** were reduced to the corresponding diols **28a** and **28b** using $LiAlH_4$. Cyclization of these diols **28a-b** with methylpyruvate in the presence of $BF_3.OEt_2$ gave the cyclized compounds as a mixture of *cis* and *trans* isomers which were separated by column chromatography to obtain the *cis* isomers **29a-b** as the major products. Debenzylation of **25f**, **29a** and **29b** under transfer hydrogenation conditions employing Pd/C and ammonium formate in methanol giving the corresponding hydroxy compounds **25i**, **30a** and **30b** which were treated with methanesulfonyl chloride and triethylamine in dichloromethane to yield the compounds **25j**, **31a** and **31b** respectively. Hydrolysis of these compounds under aqeuous basic condition followed by neutralization gave the acids **26j**, **32a** and **32b**.

Scheme 10:

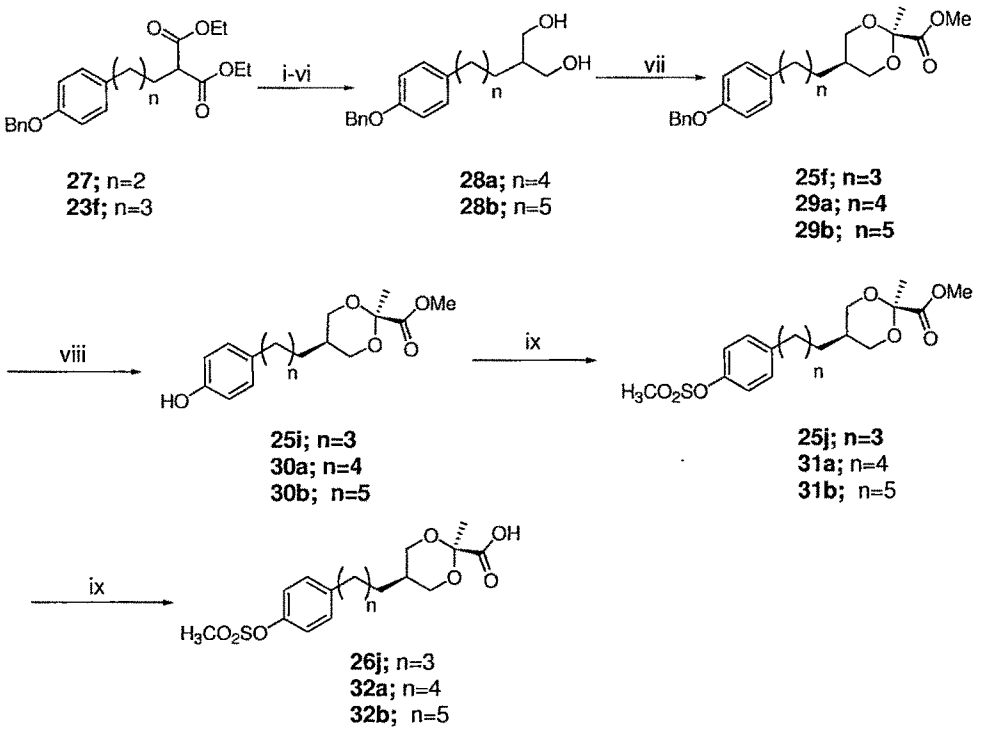

Reagents and Conditions: (i) NaOH, EtOH, H_2O, 25 °C, 18 h; (ii) AcOH, xylene, reflux, 4 h; (iii) $LiAlH_4$, THF, 0-10 °C, 1 h; (iv) CH_3SO_2Cl, Et_3N, CH_2Cl_2, 0-10 °C, 30 min; (v) Diethyl malonate, NaH, THF, 60 °C, 48 h; (vi) $LiAlH_4$, THF, 0-10 °C, 1 h (vii) $MeCOCO_2Me$, $BF_3.OEt_2$, CH_3CN, 25 °C, 2 h; (viii) $HCOONH_4$, Pd/C (10%), MeOH, reflux, 2 h; (ix) LiOH, H_2O, THF, MeOH, 25 °C, 18 h.

3.2.2. Biology

Initial compounds **26a-j** were designed by hybridizing the structures of NS-220 and K-111 wherein the phenyl ring is connected with 1,3-dioxane acidic head with an alkyl tether. Phenyl ring has been substituted at *para*-position as the activity of these compounds is sensitive to substituent at this position. *in vitro* hPPAR transactivation is reported here as fold induction and their ability to reduce serum triglycerides (TG) in male *Swiss albino mice* (SAM), which is a moderately hyperlipidemic model, and the results are shown in **Table 12.**

Table 12

in vitro hPPAR transactivation and TG lowering activity of **26a-j**

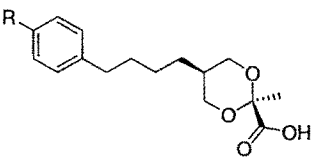

Compound	R	hPPAR Transactivation[a]			% Change in TG in SAM[b]
		α (10μM)	γ (0.2μM)	δ (10μM)	
26a	Me	3.2	1.5	1.1	-22
26b	F	2.3	2.1	1.2	-9
26c	SMe	4	1.9	1.9	-14
26d	OMe	2.5	1.2	1.2	-11
26e	Cl	2.6	2.2	2.2	-10
26f	OBn	2.3	1.0	1.0	-25
26g	SOMe	2	1.8	1.8	-12
26h	SO_2Me	1	2.2	2.2	-7
26i	OH	1.2	1.4	1.4	-15
26j	OSO_2Me	3.0	1.0	1.0	-32
Vehicle		1.0	1.0	1.0	0.0
WY-14643		3.3	ND	ND	ND
Rosiglitazone		ND	10.2	ND	ND
GW-501516		ND	ND	5.6	ND

[a] hPPAR denotes human PPAR. Activities are presented as fold induction of PPARα, γ and δ activation over the basal level (DMSO). ND denotes not determined.

[b] Values indicated are the mean of n=6 animals and $p < 0.05$ vs vehicle control

Compounds **26a** and **26j** showed around 3 fold activation above basal level (activation shown by DMSO) towards PPARα. All other compounds did not show activation comparable to WY-14643. None of the compounds showed activation towards PPARγ andδ. **26j** also reduced serum triglycerides (TG) by 32%, while the other compounds were found to exhibit inferior activity *in vivo*. These results reveal that the substitution at *para* position on the phenyl ring contributes significantly to the *in vitro* as well as *in vivo* triglyceride lowering

activity of these compounds. Based on these results **26j** was selected for further modifications.

We fixed the tail group as *para* methanesulfonyloxy phenyl group and opted to optimize the tether length. Compounds **32a** and **32b** were synthesized by elongating the tether length to five carbons and six carbons respectively. PPAR *in vitro* activity of these compounds (**32a-b)** and their TG lowering activity in SAM model are summarized in **Table 13**.

Table 13

in vitro hPPAR transactivation and TG reducing activity of compounds **26j, 32a & 32b**

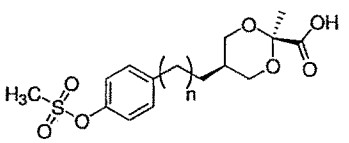

Compound	n	hPPAR transactivation (EC_{50} μM)		% Change in TG in SAM[b]
		α	γ	
26j	3	20	IA	-32
32a	4	2.5	IA	-28
32b	5	2	15	-71
NS-220		0.05	7	-67
Tesaglitazar		0.82	0.013	-79

[b]Values indicated are the mean of n=6 animals and $p < 0.05$ vs vehicle control

Compound **32a** containing pentyl chain as tether found inferior to **26j** but surprisingly compound **32b** containing hexyl chain as tether reduced serum TG significantly (71%). The transient transactivation results of these compounds are reported as EC_{50} (**Table 13**) which shows that the compound **32b** is a moderate activator of PPAR. Having surprised and encouraged with the initial results of compound **32b,** we evaluated it in *db/db* mice and high cholesterol fed *Sprague Dawley* rats (HC fed SD rats). In *db/db* mice model **32b** showed excellent serum glucose and TG reduction which are comparable to NS-220 (**Table 14**).

Treatment of high cholesterol fed *Sprague Dawley* rats (HC fed SD rat) with compound **32b** reduced TG by 63% and serum cholesterol (TC) by 56% Additionally treatment with **32b** resulted in 46% reduction in low density lipoprotein cholesterol (LDL-C) and 51% increase in high density lipoprotein cholesterol (HDL-C) (**Table 15**).

Table 14

Hypoglycemic and hypolipidemic activities of compound **32b** in *db/db* mice[a]

Compound	Dose (mg/kg/day)	% Change	
		TG	Glucose
32b	3	-50	-53
NS-220	3	-54	-44
Tesaglitazar	3	-60	-54

[a]Values indicated are the mean of n=6 animals and $p < 0.05$ vs vehicle control

Table 15

Hypolipidemic activity of compound **32b** in HC fed SD rats[a]

Compound	Dose (mg/kg/day)	% Change			
		TG	TC	LDL-C	HDL-C
32b	3	-63	-56	-46	51
NS-220	3	-54	-49	-68	88
Tesaglitazar	3	-51	-59	-31	18

[a]Values indicated are the mean of n=6 animals and $p < 0.05$ vs vehicle control

To understand further and to draw correlation between moderate *in vitro* potency and high *in vivo* efficacy of compound **32b,** its pharmacokinetic parameters were evaluated and presented in **Table 16**. Compound **32b** showed C_{max} of 127 μg/mL and an AUC of 1491 h.μg/mL when administered orally to male *Wistar* rat at a dose of 30 mg/kg body weight. These results clearly

established the compound **32b** as a highly efficacious and bioavailable hypoglycemic and hypolipidemic agent with moderate *in vitro* potency.

Table 16

Mean pharmacokinetic parameters[a] of **32b** in fasted male *Wistar* rat

Compound	Route	dose (mg/kg)	T_{max} (h)	C_{max} (μg/mL)	$T_{1/2}$ (h)	AUC(0-∞) (h.μg/mL)
32b	Oral	30	4	127	12	1491
NS-220	Oral	30	0.67	41	1.5	99

[a] Values indicated are the mean of n=6 animals and $p < 0.05$ vs vehicle control

3.3. Modulation of subtype selectivity: Converting PPARα/γ dual agonists to selective PPARα agonists [222]

Since the compound **32b** was efficacious in animal models while poor activator of PPARα, we intended to derive chemical tools to modulate the activity of compounds towards PPAR sub types. Structural comparison of our lead PPARα/γ dual agonist **15b** with a contemporarily reported PPARα agonist **NS-220** led to an interesting observation. These two compounds differ structurally in spacer region *i.e.* the compound **15b** possesses the aromatic phenylene spacer and found to be PPARα/γ dual agonist, whereas **NS-220** possesses an alkyl chain as a spacer between the acidic head and the lipophilic tail and is a selective PPARα agonist. Based on these observations we envisioned that PPAR subtype selectivity of ligands may be sensitive to chemical variations in the spacer region of the structure and further hypothesized that replacing an aromatic spacer of a PPARα/γ dual agonist with an alkyl one may convert it to a selective PPARα agonist. To validate our hypothesis we intended to study the effect of changing the aromatic phenylene spacer of Imiglitazar and Muraglitazar to a polymethylene spacer in order to develop selective PPARα agonist. Compounds represented by general structures **39** and **42** with varying length of alkyl spacer were designed.

3.3.1. Chemistry

Synthesis of compounds **39** and **42** is depicted in **Schemes 11-13** below.

Scheme 11:

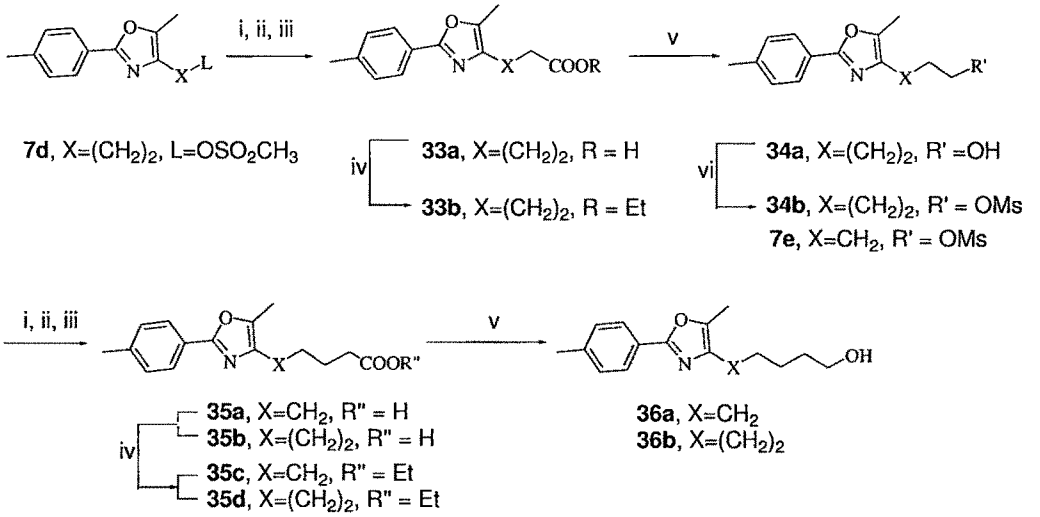

Reagents and Conditions: (i) Diethyl malonate, NaH, DMF, 25 °C, 18 h; (ii) aq. NaOH, MeOH, 25 °C, 0.25 h; (iii) Xylene, reflux, 5 h; (iv) EtOH, H_2SO_4, Reflux, 24 h; (v) $LiAlH_4$, THF, 25 °C, 0.5 h; (vi) CH_3SO_2Cl, Et_3N, CH_2Cl_2, 10 °C, 0.25 h.

Synthesis of the intermediate hydroxy compounds **34a** and **36a-b** is illustrated in **Scheme 11**. Treatment of **7d** with diethylmalonate in presence of sodium hydride followed by the hydrolysis of the diester and decarboxylation under thermal conditions gave the carboxylic acid **33a**. Esterification of the acid **33a** to **33b** followed by reduction of the ester with $LiAlH_4$ gave the hydroxy compound **34a.** Treatment of **34a** with methanesulfonylchloride and triethylamine gave the mesylate derivative **34b**. Mesylate derivatives **34b** and **7e** were subjected again to the same series of reactions as mentioned above to elongate the chain and obtain the acids **35a** and **35b** respectively. Esterification of these acids to their corresponding esters **35c** and **35d** followed by the reduction using $LiAlH_4$ gave the hydroxy compounds **36a** and **36b**.

Compounds **39a-c** were synthesized according to **Scheme 12**. The hydroxy compounds **34a, 36a** and **36b** were oxidized to the corresponding

aldehydes **37a-c** with pyridiniumchlorochromate in dichloromethane and were reacted with glycine ethyl ester under reductive amination conditions followed by acylation of the intermediate with 4-methoxyphenylchloroformate to yield the ester **38a-c**. Hydrolysis of **38a-c** under aqueous basic conditions followed by neutralization furnished the acid derivatives **39a-c**.

Scheme 12:

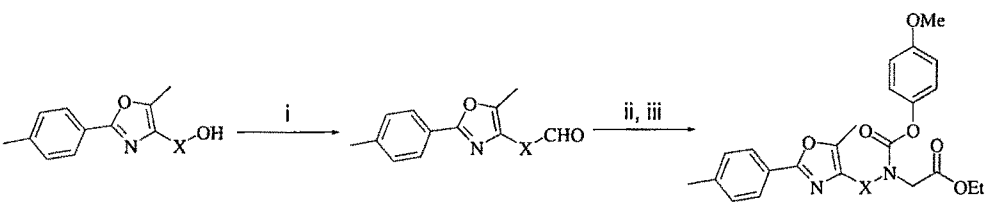

34a, X=$(CH_2)_4$
36a, X=$(CH_2)_5$
36b, X=$(CH_2)_6$

37a, X=$(CH_2)_3$
37b, X=$(CH_2)_4$
37c, X=$(CH_2)_5$

38a, X=$(CH_2)_4$
38b X=$(CH_2)_5$
38c, X=$(CH_2)_6$

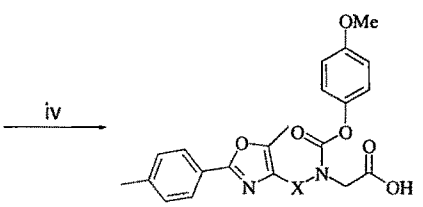

39a, X=$(CH_2)_4$
39b, X=$(CH_2)_5$
39c, X=$(CH_2)_6$

Reagents and condition: (i) PCC, Celite, CH_2Cl_2, 25 °C, 2 h; (ii) Glycine ethyl ester hydrochloride, MeOH, $NaBH(OAc)_3$, 25 °C, 1.5 h; (iii) 4-methoxyphenylchloroformate, CH_2Cl_2, 25 °C, 2 h; (iv) LiOH, THF, H_2O, MeOH, 25 °C, 3 h.

Synthetic strategy for the compounds **42a-c** is outlined in **Scheme 13**. The hydroxy compounds **34a** and **36a-b** were converted to their mesylate derivatives **34b** and **40a-b** respectively followed by coupling with compound **44** in the presence of base to obtain the corresponding esters **41a-c** which were hydrolyzed with aqueous base followed by neutralization to afford the acids **42a-c**.

Scheme 13:

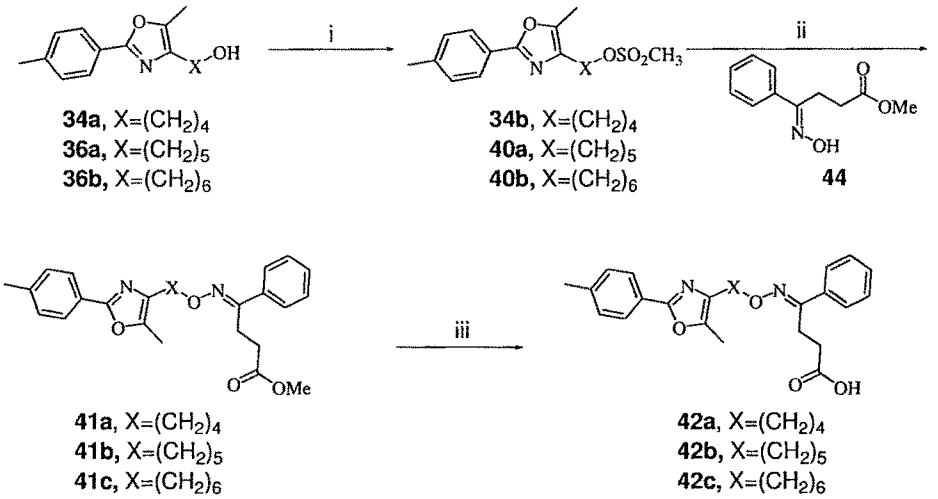

34a, X=$(CH_2)_4$
36a, X=$(CH_2)_5$
36b, X=$(CH_2)_6$

34b, X=$(CH_2)_4$
40a, X=$(CH_2)_5$
40b, X=$(CH_2)_6$

44

41a, X=$(CH_2)_4$
41b, X=$(CH_2)_5$
41c, X=$(CH_2)_6$

42a, X=$(CH_2)_4$
42b, X=$(CH_2)_5$
42c, X=$(CH_2)_6$

Reagents and conditions: (i) CH_3SO_2Cl, Et_3N, CH_2Cl_2, 10 °C, 0.25 h; (ii) NaH (50%), DMF, 60 °C, 24 h; (iii) LiOH, THF, H_2O, MeOH, 25 °C, 5 h.

3.3.2. Biology

Analysis of transient transactivation activity of the compounds towards hPPARα and γ was determined (as EC_{50}), and the results are summarized in **Table 17**. The transactivation results with the compounds **39a-c** were although not convincing but encouraging as we observed that replacing the phenoxy spacer of Muraglitazar with the alkyl chain made the compound **39b** less potent towards PPARγ compared to PPARα increasing the γ to α ratio of EC_{50} to 12 against 0.6 as in case of Muraglitazar whereas the compound **39c** did not show any selectivity towards PPARα. Encouraged with these results and in urge of potent and highly selective PPARα agonist, the compounds **42a-c** were synthesized taking Imiglitazar as initial lead this time. The transactivation results of the compounds **42a-c** were found very convincing and were in line with our hypothesis. Compounds **42a** and **42c** are found very potent and selective PPARα agonists with picomolar and nanomolar range EC_{50} respectively and multi-fold selectivity towards PPARα over PPARγ whereas compound **42b** showed inferior results in terms of selectivity towards PPARα transactivation. Finally *in vitro* profile of **15b** and **NS-220** are also found to be in support of our

hypothesis as the former with the phenylene spacer exhibits dual agonism whereas the latter with tetramethylene spacer is a selective PPARα agonist.

Table 17

in vitro hPPAR transactivation activity of **39, 42** and **15b**.

Compound	hPPAR Transactivation EC_{50} (μM)[a]			
	α	γ	Ratio γ/α	δ
39a	IA	IA	-	IA
39b	0.044	0.56	12	IA
39c	0.034	0.45	13	IA
42a	0.0000038	0.43	113157	IA
42b	0.002	0.031	15	IA
42c	0.0001	0.1	1000	IA
15b	0.072	0.015	0.2	IA
Imiglitazar	0.008	0.004	0.5	IA
Muraglitazar	0.15	0.09	0.6	IA
NS-220	0.052	6.85	131	IA

[a] hPPAR denotes human PPAR. IA denotes inactive where compounds did not show any fold induction above the basal level shown by vehicle.

3.3.3. Molecular docking study

Molecular docking simulations were carried out for **42a** and Imiglitazar using same protocol as described earlier. When docked into PPARα binding pocket, both **42a** and Imiglitazar adopted a conformation that allows the carboxylic group to form hydrogen bonds with Tyr314, Tyr464 and Ser280. (**Figure 23**)

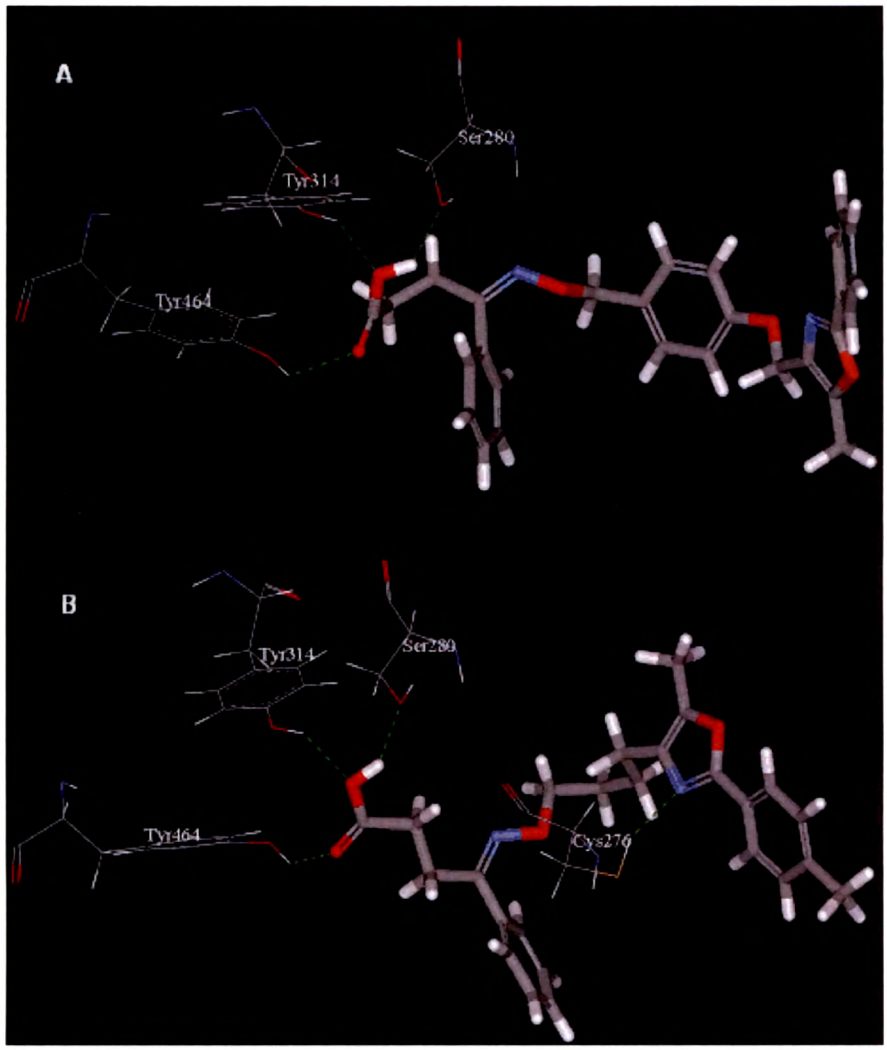

Figure 23. Imiglitazar (**A**), **42a** (**B**) docked into PPARα binding site. *H*-bond interactions with amino acids are shown as dashed lines.

However in the docking model of **42a** an additional *H*-bond between the nitrogen atom of oxazole ring and Cys276 was observed. This additional H-bond may actually be responsible for improved activity of this compound over Imiglitazar. **42a** when docked into PPARγ binding pocket none of the conformations showed H-bond interactions with any of the amino acids though the molecular orientation was similar to that of Imiglitazar which correlates with a moderate PPARγ activity of this compound whereas Imiglitazar showed H-bond

interactions with Cys295 while Ser289 and Tyr473 lying in close proximity of the ligand.

3.4. Bisoximinoalkanoic acid derivatives as potent and selective PPARα agonists [223]

Even though **42a** exhibits a high degree of selectivity towards PPARα overγ, its picomolar potency raises concerns of possible toxicity for further development of this compound. In order to study PPARα selective agonists further based on compound **42a**, molecular modeling experiments were undertaken and based on the results (data not shown) we envisioned that replacement of rigid oxazole heterocycle with a flexible bioisostere would be a good strategy and designed a novel series of bisoximinoalkanoic acid derivatives centering the modifications in lipophilic tail as depicted in the **Figure 24.**

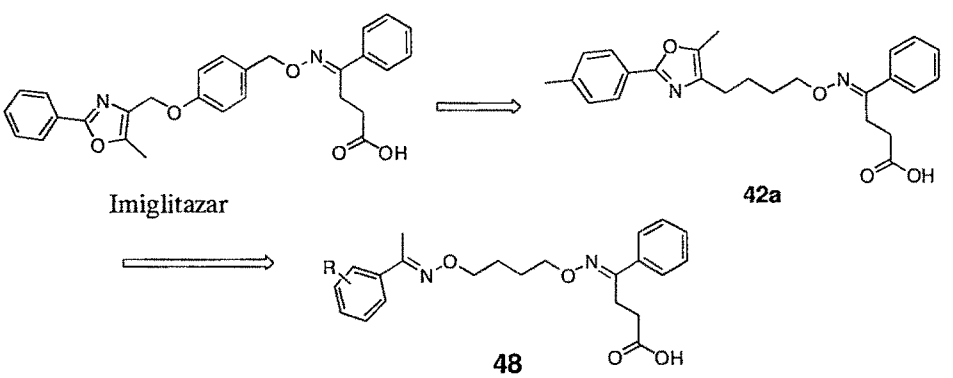

Figure 24. Designing selective PPARα agonist

3.4.1. Chemistry

Synthesis of the compounds **48** is depicted in **Schemes 14** and **15.**

Synthesis of intermediate **45** was depicted in **Scheme 14.** Intermediate **43** was synthesized by the Friedel-Crafts acylation of benzene with succinic anhydride. Treatment of **43** with hydroxylamine hydrochloride gave the oxime derivative as a mixture of *E* and *Z*- isomers and the *E*- isomer **44** was isolated by column chromatography as a major product which showed ^{1}HNMR chemical

shifts identical with reported values [**224**]. Alkylation of **44** with 1,4-dibromobutane gave the intermediate **45** in a good yield.

Scheme 14:

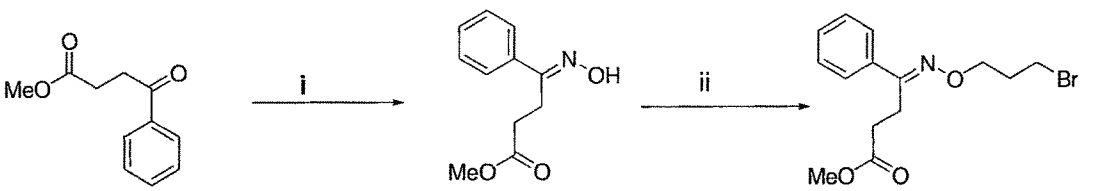

43 **44** **45**

Reagents and conditions: (i) Hydroxylammonium chloride, NaOAc, EtOH, reflux, 2h; (ii) 1,4-dibromobutane, K_2CO_3, DMF, 60 °C, 24 h.

Scheme 15:

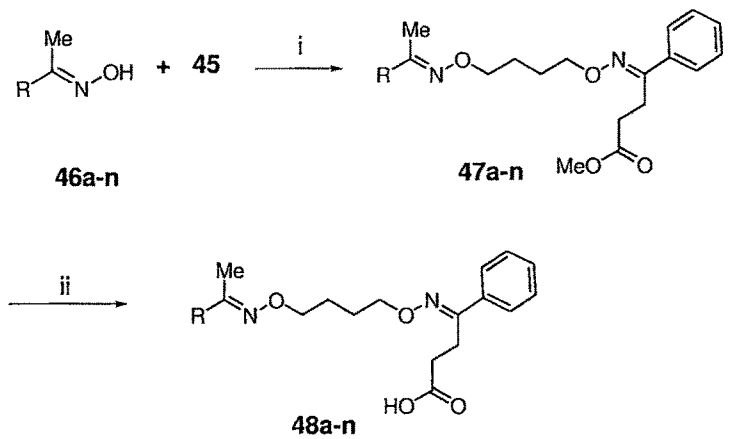

46a-n **47a-n** **48a-n**

	R
a	phenyl
b	4-fluorophenyl
c	4-methylphenyl
d	4-methoxyphenyl
e	4-trifluoromethylphenyl
f	4-methanesulfonylphenyl
g	4-(*n*-butyl)phenyl
h	1,1'-biphenyl-4yl
i	2-napthyl
j	1,2,3,4-tetrohydronaphthalen-6yl
k	3,4-dimethoxyphenyl
l	3,4-dimethylphenyl
m	3-methoxy-4-methylphenyl
n	4-fluoro-3-methoxyphenyl

Reagents and conditions: (i) K_2CO_3, DMF, 60 °C, 8 h; (ii) NaOH, H_2O, MeOH, 25 °C, 18 h.

Synthesis of the compounds **48a-n** is presented in **Scheme 15**. The oximes **46a-n** were synthesized by reacting the corresponding acetophenone with hydroxylamine hydrochloride giving *E*-isomers as they are thermodynamically more stable than *Z*-isomers [**218**]. Coupling reaction between intermediate **45** and **46a-n** under basic conditions gave the ester derivatives **47a-n** which upon hydrolysis under aqueous basic condition followed by neutralization gave the acids **48a-n**.

3.4.2. Biology

Compounds **48a-n** were screened for hPPARα, γ and δ agonistic activities on full length PPAR receptor transfected in HepG2 cells. WY-14643, Rosiglitazone and GW-501516 were used as controls for PPARα,γ and δ respectively and the results are summarized in **Table 18** where the activities are shown as EC_{50}. None of the compounds show any fold induction above the basal level (shown by vehicle) up to 1μM concentration towards PPARδ. Triglyceride lowering activity was measured by administering the compounds orally at a dose of 10 mg/kg/day for 6 days to male *Swiss albino* mice (SAM) which are moderately hyperlipidemic. Values reported are the % change in serum triglyceride (TG) concentration of the compound-treated mice relative to vehicle controls and are summarized in **Table18**. Our goal was to develop potent and selective PPARα agonist that do not contain phenyloxazole group starting from compound **42a** described in the previous section. Compounds **48** were designed by replacing the oxazole ring with an oximino group expecting it to behave as a bioisostere of oxazole and synthesized the compounds **48a-n**. As the initial compound **48a** was found to be inactive, we envisioned based on our experience that substitution at metabolically susceptible *para* position of phenyl ring of tail part may play an important role in the modulation of potency and selectivity of the compounds which became evident from the *in vitro* activity of **48b**. Compounds **48c** and **48d** with electron releasing methyl and methoxy groups respectively were found to be potent and selective towards PPARα. **48d** exhibited 110 fold selectivity towards PPARα over γ and reduced serum triglycerides by 35% in the SAM model whereas **48c** though exhibited potency similar to **48d** *in vitro* did not show significant TG reduction *in vivo*. Substitution on this position with electron-withdrawing groups exhibited detrimental effects both *in vitro* and *in vivo*, which is evident from the activity of **48e** and **48f** possessing trifluoromethyl and methanesulfonyl groups respectively. We then intended to study the effect of bulky substituents on the phenyl ring. **48g**, with the *n*-butyl group, was found to be a weak activator of PPARα and γ with an EC_{50} of 0.5 and 0.2 μM respectively.

To our surprise this compound reduced TG by 31%. Further increase of the bulk at this position by introducing a phenyl ring made the compound **48h** a potent activator of PPARα but found to be only 5 fold selective over PPARγ. Replacing the flexible *n*-butyl chain with a rigid group by fusing the 3 and 4 positions into a naphthyl or tetrahydronaphthyl group gave the compounds **48i** and **48j** respectively, which showed surprising and interesting results. **48i** and **48j** are found to be equipotent towards PPARγ. **48i** exhibits 6 fold selectivity towards PPARα over PPARγ and reduces TG by 25% *in vivo* whereas **48j** is found to be 10 fold more potent than **48i** towards PPARα and shows 36% reduction in TG. These results suggested that increasing the bulk of the lipophilic tail increases the affinity of the compounds towards PPARγ and guided us to study the effect of substituents on both 3- and 4- positions of the phenyl ring. Since electron releasing groups appeared to be favorable, we chose methoxy and methyl as well as electron withdrawing fluoro groups and synthesized the compounds **48k**, **48l**, **48m** and **48n**. Among these compounds **48k** and **48n** showed weak and equal affinity towards PPARα and γ but **48k** reduced TG by 30% *in vivo* whereas **48n** did not show significant reduction in TG. **48l** with two methyl groups found to be the most potent and highly selective towards PPARα with an EC_{50} of 0.002 μM and 500 fold selectivity over PPARγ. But this compound is not efficacious in reducing TG *in vivo*. **48m** with methoxy group at *meta* position and methyl group at *para* position exhibited similar potency and selectivity as **48l** *in vitro* with an EC_{50} of 0.005 μM towards PPARα and 320 fold selectivity over γ. This compound reduced TG by 36% *in vivo*. **48d** and **48m** were identified as the lead compounds for further evaluation.

Table 18

in vitro hPPAR transactivation and TG lowering activity of **48a-n**

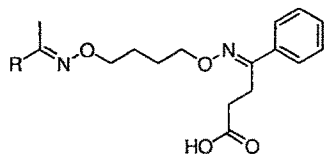

Compound	R	hPPAR transactivation[a]					% Change in TG in SAM[c]
		α^b (10μM)	γ^b (0.2μM)	δ^b (10μM)	$EC_{50}\alpha$ (μM)	$EC_{50}\gamma$ (μM)	
48a		2.9	IA	IA	2.3	IA	ND
48b		5.2	6.8	IA	0.05	1.4	-18
48c	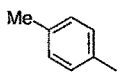	4.3	6.8	1.9	0.05	2.1	-13
48d	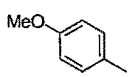	5.2	2.0	IA	0.01	1.1	-35
48e	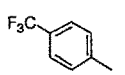	4.3	4.1	2.4	0.4	1.4	-0.6
48f	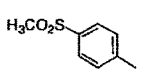	2.7	5.1	IA	2.4	1.9	-14
48g	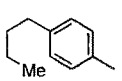	4.6	6.4	1.4	0.5	0.2	-31
48h	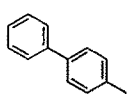	4.5	5.3	2.1	0.02	0.1	-23
48i	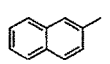	3.6	5.2	1.7	0.03	0.2	-25
48j	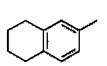	4.6	6.1	1.6	0.003	0.2	-36
48k	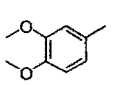	6.7	4.8	1.8	0.1	0.8	-30
48l	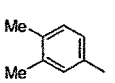	4.7	5.0	1.9	0.002	1.0	-12
48m	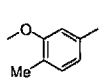	11.8	6.0	1.4	0.005	1.6	-36
48n	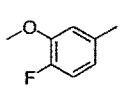	6.1	7.3	1.8	0.4	0.7	-19

Compound	R	hPPAR transactivation[a]					% Change in TG in SAM[c]
		α^b (10μM)	γ^b (0.2μM)	δ^b (10μM)	$EC_{50}\alpha$ (μM)	$EC_{50}\gamma$ (μM)	
Imiglitazar		6.1	8.5	3.2	0.005	0.004	-37.4
Vehicle		1.0	1.0	1.0			-
WY-14643		5.2	ND	ND	4.8	ND	ND
Rosiglitazone		ND	9.4	ND	ND	0.05	ND
GW-501516@ 2 nM		ND	ND	4.8	ND	ND	ND

[a] IA denotes inactive where compounds did not show any fold induction above the basal level shown by vehicle and ND denotes not determined. hPPAR denotes human PPAR.

[b] Activities are presented as fold induction of PPARα, γ and δ activation over the basal level (DMSO).

[c]Values indicated are the mean of n=6 animals and $p < 0.05$ vs vehicle control.